

# **SURFACE AND INTERFACE PROPERTIES OF PVDF/ACRYLIC COPOLYMER BLENDS BEFORE AND AFTER UV EXPOSURE**

by

**X. Gu, L. Sung, D.L. Ho, C.A. Michaels, T. Nguyen**  
National Institute of Standards and Technology  
Gaithersburg, MD 20899 USA

**D. Nguyen**

**PPG Industries, Inc.**  
Allison Park, PA

**And**

**Y.C. Jean**

**University of Missouri-Kansas City, Kansas City, MO**

Reprinted from the Proceedings of the 80<sup>th</sup> Annual Meeting Technical Program of the FSCT,  
Oct. 30-Nov. 1, 2002, Ernest N. Morial Convention Center, New Orleans, LA. Publisher:  
Federation of Societies for Coatings Technology, 492 Norristown Rd., Blue Bell, PA 19422 USA.

**NOTE:** This paper is a contribution of the National Institute of Standards and Technology  
and is not subject to copyright.



**NIST**

**National Institute of Standards and Technology**  
Technology Administration, U.S. Department of Commerce

# **SURFACE AND INTERFACE PROPERTIES OF PVDF/ACRYLIC COPOLYMER BLENDS BEFORE AND AFTER UV EXPOSURE**

*X. Gu<sup>1,2</sup>, L. Sung<sup>1</sup>, D.L. Ho<sup>1</sup>, C.A. Michaels<sup>1</sup>  
D. Nguyen<sup>3</sup>, Y.C. Jean<sup>2</sup>, and T. Nguyen<sup>1</sup>*

<sup>1</sup>*National Institute of Standards and Technology, Gaithersburg, MD*

<sup>2</sup>*University of Missouri-Kansas City, Kansas City, MO*

<sup>3</sup>*PPG Industries, Inc., Allison Park, PA*

## **Introduction**

Poly(vinylidene fluoride) (PVDF)-based coatings are increasingly used for protecting outdoor structures. Due to the unique structure of PVDF, these coatings exhibit excellent chemical resistance, outstanding gloss retention, good flexibility, and renowned ability to resist chalking and cracking during weathering.<sup>1</sup> It has been reported that PVDF resins have a 35-year history of outstanding performance in outdoor application.<sup>2</sup> Weathering test in Florida also showed that the gloss of PVDF coatings increased by 15% over four years when a typical acrylic coating exhibited a 60% decrease in gloss over the same period.<sup>3</sup> However, the chemical inertness of PVDF prevents good adhesion to substrates and makes it difficult to disperse pigments. Other disadvantages of PVDF coatings, such as inability to produce a glossy finish, high melt viscosity, inferior scratching and marring resistance and high cost, make it indispensable to introduce a secondary polymer component to optimize the performance of PVDF materials.<sup>4</sup> The most widely used class of polymers is acrylic resin, such as poly(methyl methacrylate) (PMMA) and its copolymers. These polymers have not only good compatibility with PVDF but also provide good heat resistance, mechanical properties, weatherability and optical clarity.

The preparation methods and the process conditions strongly influence the microstructure and morphology of coatings and, hence, their durability. Generally, the acrylic modifier is physically blended with the PVDF resin in solvent (usually isophorone). Oven heating at 230 °C or above causes the solvent to be completely removed and allows PVDF to melt and film formation to occur. Molten PVDF is miscible with some acrylic polymers, such as PMMA, at a wide temperature range. The mixture tends to phase separate at temperature above the lower critical solution temperature (LCST) around 350 °C.<sup>5</sup> Below the melting temperature  $T_m$  (~178 °C), PVDF crystallizes from the homogeneous melt.<sup>6</sup> This physical blending produces a PVDF/acrylic mixture on a macro-molecular scale.<sup>1</sup> Some novel approaches have been developed to mix the fluoro and acrylic polymers on a micro-molecular scale. The process is based on incorporating the acrylic with the fluoropolymer in the polymerization stage such as during emulsion polymerization process.<sup>1</sup> This process has reportedly produced coatings with significantly improved properties and can be easily achieved in water-borne coatings.

The surface and interface properties of a coating system have a strong influence on its service life and its adhesion to the substrate. Extensive research has experimentally demonstrated that the surface structure of a polymer blend tends to be different from that in the bulk due to the difference in the

surface free energy of each component.<sup>7,8</sup> A previous investigation of PVDF blended with various amorphous polymers has shown that the concentration of PVDF present at the air surface is greater than that in the bulk.<sup>9</sup> Such surface enrichment has also been observed for fluorochemical-doped polymers and other polymer blends.<sup>10,11</sup> In addition to chemical enrichment, the crystallinity at the surface of some homopolymers is enhanced.<sup>12</sup> On the other hand, the buried interface/interphase between a coating and a substrate is often affected by the properties of the substrate and the processing conditions that control the chemical kinetics, diffusion, and volumetric changes. Therefore, the chemical, physical, and mechanical properties in the interface region could be different from the bulk or the surface. Although much work has addressed the phase separation and crystallization of PVDF/acrylic polymers blend films, little is known about their surface and interface properties, such as microstructure, morphology and chemical compositions, particularly the change of these properties when the films are exposed to ultraviolet (UV) irradiation. Such data would provide a better understanding on the service life of PVDF-based coatings with respect to the surface properties such as gloss, wettability, and weatherability, and the interfacial properties such as adhesion and delamination.

The main objective of this study is to investigate the morphology/microstructure and chemical composition of both the surface and the interface of films prepared from blends of PVDF with a copolymer of PMMA and poly(ethyl acrylate) (PMMA-co-PEA) before and after UV exposure. Surface and interface morphologies were studied by atomic force microscopy (AFM). Chemical composition information was obtained by attenuated total reflection-FTIR spectroscopy (ATR-FTIR), contact angle measurements, and novel confocal Raman microscopy technique. To obtain the microstructure of the bulk, small angle neutron scattering (SANS) was used.

## **Experimental Procedures\***

### ***Materials and Sample Preparation***

PMMA-co-PEA solutions in toluene were thoroughly mixed with PVDF powders to provide desired blends by gradually adding isophorone solvent under electric stirring. The mass ratios between PVDF and PMMA-co-PEA were 70/30, 50/50 and 30/70. The mixtures were cast on glass plates by a drawdown technique to provide a dry film thickness of approximately 75  $\mu\text{m}$ . After heating at 246  $^{\circ}\text{C}$  for 10 min in an air-circulated oven, coated glass plates were removed from the oven and slowly cooled to ambient temperature (24  $^{\circ}\text{C}$ ). After immersing in boiling water for 10 min, the films were readily peeled from the glass plates. The film side that was exposed to the air during film formation is termed the “surface”, while the other side contacted with the glass substrate is designated as the “interface”. Surface and interface samples were characterized before and after exposure to UV light at 50  $^{\circ}\text{C}$  and 9 % relative humidity (RH) for 7 months. The radiation source of UV light was supplied by a 1000 W xenon arc solar simulator, which provides infrared-free, near ambient temperature (24  $^{\circ}\text{C}$ ) radiation with wavelengths between 275 nm and 800 nm.

### ***Atomic Force Microscopy (AFM)***

A Dimension 3100 Scanning Probe Microscope from Digital Instruments was operated in tapping mode to characterize the surface and interface morphology of PVDF/PMMA-co-PEA blend films

before and after UV exposure. Commercial silicon microcantilever probes were used. Topographic and phase images were obtained simultaneously using a resonance frequency of approximately 300 kHz for the probe oscillation and a free-oscillation amplitude of  $62 \text{ nm} \pm 2 \text{ nm}$ . The set-point ratio (the ratio of set point amplitude to the free amplitude) ranged from 0.60 to 0.80.

### ***Confocal Raman Microscopy***

Confocal Raman microscopy is a novel tool for the non-destructive characterization of materials utilizing the chemical specificity of Raman scattering spectroscopy. The attainable lateral spatial resolution is limited only by diffraction and thus can be sub-micrometer for excitation at visible wavelengths. Incorporation of the optical sectioning capabilities of confocal microscopy yields outstanding vertical discrimination as well, allowing depth profiling with vertical resolution in the several micrometer range. In this study, the Raman spectra were recorded on a custom confocal microscope constructed at National Institute of Standards and Technology (NIST). The excitation source was a Ti:Sapphire laser at 785 nm. The incident power at the sample was nominally 10 mW, focused to an approximately 600 nm diameter spot. The depth of focus for this system was expected to be nominally 8  $\mu\text{m}$ . The integration times used were 60 seconds for the pure compound spectra and 10 seconds for the surface and the interface spectra of the 50/50 blend sample.

### ***Small Angle Neutron Scattering (SANS)***

The microstructures of the PVDF/PMMA-co-PEA blend films in the bulk were characterized using small angle neutron scattering (SANS). SANS experiments over the  $q$  range from  $0.04 \text{ nm}^{-1}$  to  $0.9 \text{ nm}^{-1}$  were carried out using the 8-m SANS instrument at the NIST Center for Neutron Research (NCNR). The incident neutron wavelength was  $\lambda = 12 \text{ \AA}$  with a wavelength resolution of  $\Delta\lambda/\lambda = 0.15$ . The scattered intensity was corrected for background and parasitic scattering, placed on an absolute level using a calibrated secondary standard and circularly averaged to yield the scattered intensity,  $I(q)$ , as a function of the wave vector,  $q$ , where  $q = (4\pi/\lambda) \sin(\theta/2)$  ( $\theta$  is the scattering angle). The scattered intensity is proportional to the differences in the local PVDF concentration within the sample.

### ***ATR-FTIR***

ATR-FTIR analyses were performed using a diamond probe and dry air as purge gas. All ATR-FTIR spectra were the average of 132 scans at a resolution of  $4 \text{ cm}^{-1}$  using a liquid nitrogen cooled mercury cadmium telluride detector (MCT).

### ***Contact Angle Measurement***

Contact angles of water and methylene iodide on the samples were measured by the sessile droplet method. The surface free energy components, i.e., dispersion force and polar force, were calculated using the geometric mean approach. All contact angle results were the average of measurements of six drops.

## Results and Discussion

### *Morphology and Microstructure before UV Exposure*

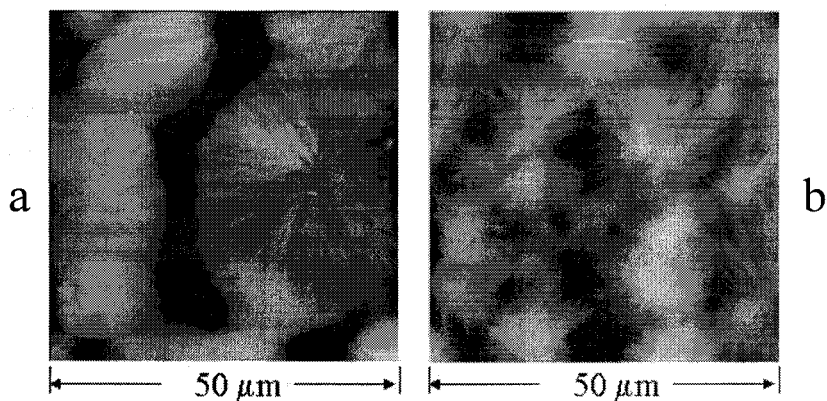


Figure 1. AFM topographic images of surface (a) and interface (b) of the 70/30 PVDF/PMMA-co-PEA blend film. The scan size is 50  $\mu\text{m}$ . Contrast variation from black to white is 1200 nm for (a) and 400 nm for (b).

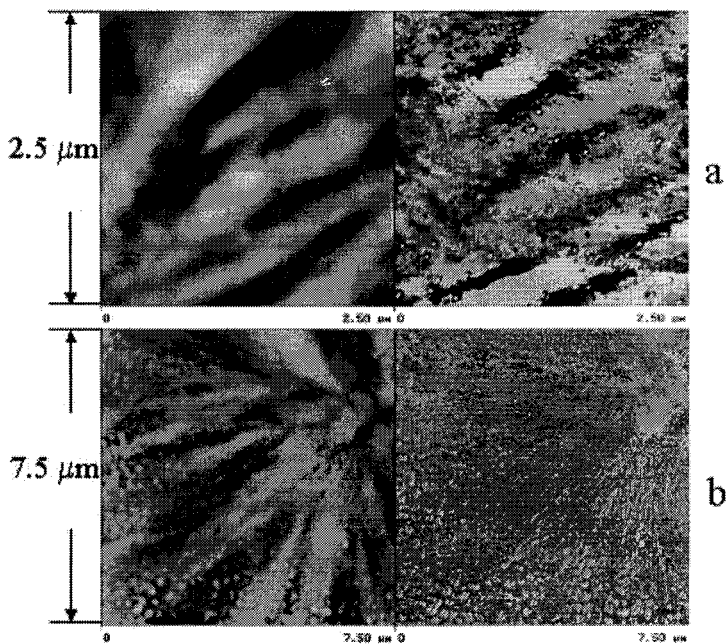


Figure 2. AFM height (left) and phase (right) images of the 70/30 PVDF/PMMA-co-PEA blend film. (a) Surface; the scan size is 2.5  $\mu\text{m}$ ; contrast variation from black to white is 50 nm for height image and 25  $^\circ$  for phase image. (b) Interface; the scan size is 7.5  $\mu\text{m}$ ; contrast variation from black to white is 50 nm for height image and 30  $^\circ$  for phase image.

AFM topographic images of the surface and the interface of the 70/30 PVDF/PMMA-co-PEA blend film are displayed in Fig.1a and Fig. 1b, respectively. One can find that both the surface and the interface exhibit typical spherulites in which aggregates of crystalline lamellae have grown from a common center in the radial direction. These visible spherulites are  $\alpha$  type of PVDF crystals.<sup>13</sup> However, there are distinct differences between the spherulites of the two sides (i.e., surface and interface) in the shape, size and distribution. The crystallites that cover almost completely on the surface are larger and circular; while those on the interface are loosely packed and less impinged. The interface is also smoother than the surface due to the smaller crystals. Fig. 2a and Fig. 2b are the higher magnifications of Fig. 1a and Fig. 1b, respectively. The left and right images of Fig. 2a and 2b correspond to the topographic and phase images, respectively. The phase images in tapping mode AFM often provide better microstructural information than the topographic images. It is interesting to notice that some particles are dispersed in the radiating branches (Fig. 2a) or aggregated in the boundaries between the crystallites (Fig. 2b). We believe that the particles are mainly PMMA-co-PEA material, because they were rejected into the inter-lamellae regions or the fronts of the spherulites during PVDF crystallization.<sup>14-16</sup> A greater number of particles is noticed on the interface than on the surface, implying that more amorphous materials (such as PMMA-co-PEA) exist on the interface. The above observations on the morphological structures indicate that the composition, the crystallinity, and/or the crystallization kinetics might be different between the surface and the interface of the blend film. The air surface of the blend may be enriched with the low surface-free energy PVDF. On the other hand, the hydrophilic nature of the glass substrate might attract the more polar acrylic copolymer, and the confined space in the interface region could constrain the crystallization of the PVDF.

It should be mentioned that, even at high magnifications, we do not observe the fine fibrils and lamella structure that was reportedly seen in the AFM images of the pure crystallized PVDF film.<sup>17</sup> However, the SANS results, as shown in Fig. 3, indicate the existence of PVDF-rich microstructure (randomly distributed lamellae structure in a three dimensional bulk film). The radius of gyration of PVDF-rich domain, which is proportional to the correlation length of PVDF concentration fluctuations, increases as the PVDF content decreases. This SANS result implies that the distance between lamellae structure increases with a higher acrylic copolymer content. Detailed explanations on neutron analyses will be reported elsewhere.<sup>18</sup> Therefore, we believe that the microstructures of the PVDF spherulites in the bulk of the blends have been modified due to the presence of the acrylic copolymer. This would occur for PVDF material on both the surface and the interface. Additionally, the incorporation of the acrylic copolymer in the crystals may have blurred the fine structure of PVDF during AFM imaging.

The morphological differences between the surface and the interface of the blend films are more evident in 50/50 PVDF/PMMA-co-PEA blend samples. Fig. 4 represents AFM topographic and phase images of the two sides of the 50/50 blend films. The surface is mostly covered with the spherulites of PVDF but the interface is void of crystal structures. Instead, the interface consists of smooth areas between 200 nm to 300 nm deep holes. High magnification images of the interface samples have revealed that the holes have an irregular shape and were actually the broken areas in the film (cohesive failure) resulting from the peeling. This observation indicates that the adhesion between the 50/50 blend film and the glass substrate was good. Evidence from the good adhesion and the absence of PVDF material on the interface suggests that amorphous PMMA-co-PEA is preferentially present at the polymer/substrate interface while PVDF enriches the surface. Similar differences are observed

between the two sides of the 30/70 blend films as shown in Fig. 5.

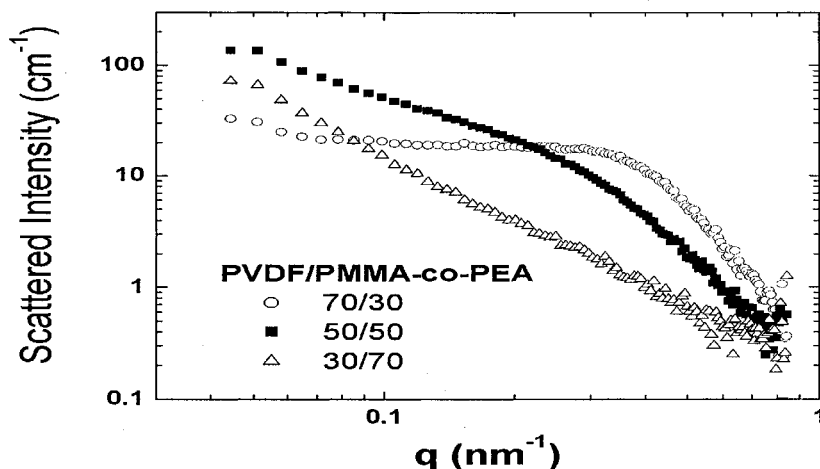


Figure 3. SANS intensity profiles of the PVDF/PMMA-co-PEA blend films at different compositions.

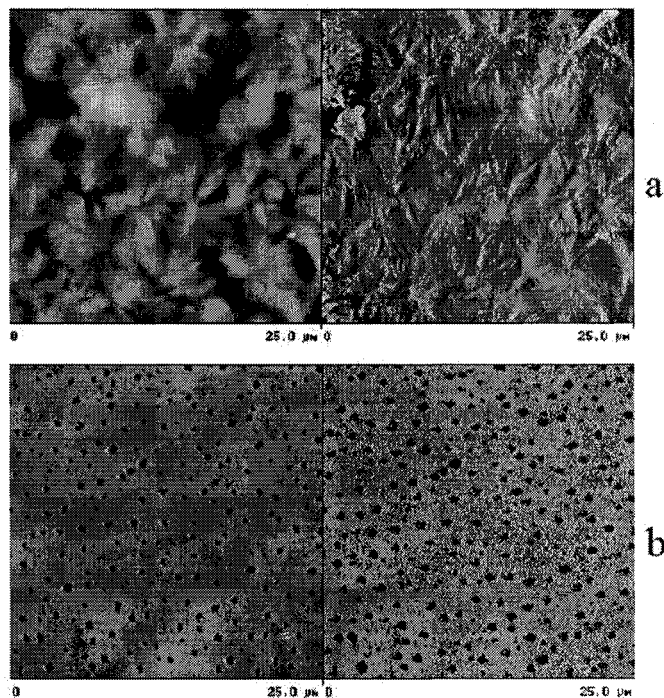


Figure 4. AFM topographic (left) and phase (right) images of surface (a) and interface (b) of the 50/50 PVDF/PMMA-co-PEA blend film. The scan size is 25  $\mu\text{m}$ . Contrast variation from black to white is 300 nm for height image and 50  $^\circ$  for phase image.

From AFM results, it can be stated that a consistent morphological difference between the surface and the interface of the three PVDF/PMMA-co-PEA blends has been observed. The surface contains more PVDF crystals and shows a rougher topography than the interface. On the other hand, the crystallization of PVDF on the interface appears to be constrained. The amorphous materials dominate the interface when the mass fraction of the acrylic copolymer in the blends is approximately  $\geq 50\%$ .

Further, one can find some relationship between the compositions of the blends with their surface and the interface microstructures. For example, the size of the spherulites on the surface of the 50/50 blends significantly drops compared to the 70/30 samples. This change may be attributed to the substantial reduction of the crystallization rate of PVDF with more amorphous PMMA-co-PEA copolymer in the mixture.<sup>19</sup> Previous study on PVDF/PMMA blends has shown that, as the concentration of PMMA increased from 0 to 50 %, the growth rate of PVDF spherulites decreased more than 100 times due to changes in melt viscosity accompanying the wide variation of  $T_g$  of the mixtures.<sup>6</sup> Our DSC analysis revealed that the 70/30 PVDF/PMMA-co-PEA blend has a  $T_g$  of 49 °C and a  $T_m$  of 157 °C; for the 50/50 blend,  $T_g$  is 53 °C and  $T_m$  is 149 °C. The increase in  $T_g$  and the decrease in  $T_m$  with higher contents of acrylic copolymer are believed to influence the crystallization rate of PVDF and, hence, the crystallite structures and the crystallinity of the blends.

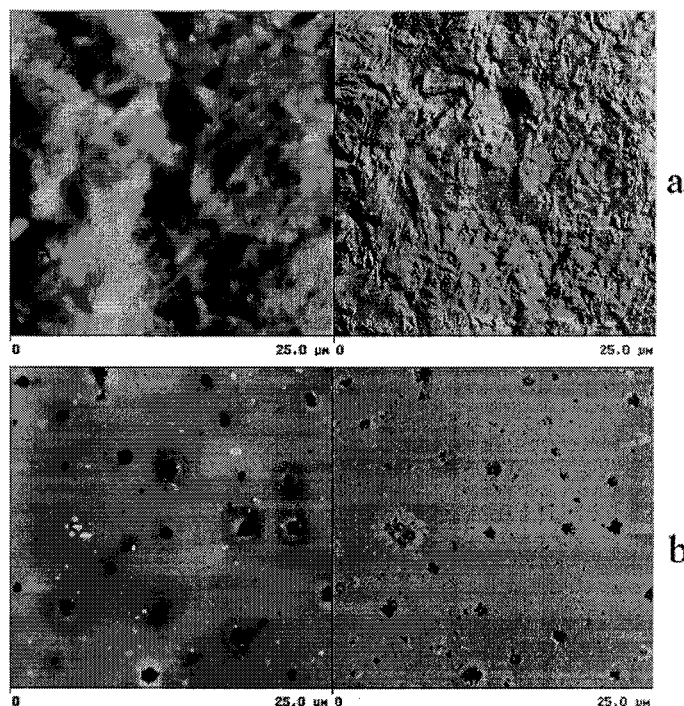


Figure 5. AFM topographic (left) and phase (right) images of surface (a) and interface (b) of the 50/50 PVDF/PMMA-co-PEA blended film. The scan size is 25  $\mu\text{m}$ . Contrast variation from black to white is 200 nm for height image and 50 ° for phase image.

### ***Chemical Composition before UV Exposure***

To verify that low surface-free energy PVDF preferentially migrated to the surface and higher surface-free energy acrylic copolymer was concentrated at the interface, confocal Raman microscopy, ATR-FTIR, and contact angle measurements of the surface and the interface samples were conducted.

Figure 6A is a plot of the Raman spectra for four samples: a pure film of PMMA-co-PEA (d), a pure film of PVDF (b), the interface side of the 50/50 blend film (c), and the surface of the 50/50 blend film (a). The cross sections for Raman scattering are clearly larger for PVDF than for the acrylic polymer and the intense  $\text{CF}_2$  stretching vibration at  $799\text{ cm}^{-1}$  is the most useful band for distinguishing between the two materials.<sup>20</sup> The spectra of the blend film have shown much greater fluorescence than the pure

compound films; the source of this emission is unknown. The blend film spectra were acquired with short integration times to assess the viability of acquiring Raman images, and thus the Raman signals are smaller than in the pure film spectra. However, comparison of the scattering intensity for the 799  $\text{cm}^{-1}$  band of the two sides of the blend film is robust and it is quite apparent that there is significantly more PVDF on the surface than on the interface. This is consistent with AFM results. Note that these measurements sample approximately the top 8  $\mu\text{m}$  of each side of the film. Figure 6B shows the same Raman spectra of the two sides of the blend film over the range 760 – 860  $\text{cm}^{-1}$  with the fluorescence background subtracted to yield a flat baseline. This subtraction procedure does not eliminate the amplitude fluctuations that are due to the shot noise on the fluorescence emission and this is the dominant source of noise in these spectra. The  $\text{CF}_2$  stretching band intensity is nominally a factor of five larger for the surface than for the interface, a difference that reflects the relative amount of PVDF at the two interfaces. The exact origin of the shoulder at 820  $\text{cm}^{-1}$  is unclear although it is likely due to a combination of a band in the acrylic copolymer at 818  $\text{cm}^{-1}$  and the tail of the  $\text{CF}_2$  stretching vibration. Depth profiling or line scans across cross-sectioned films should prove useful if mapping out the variation in PVDF concentration on going from the air to the glass interface.

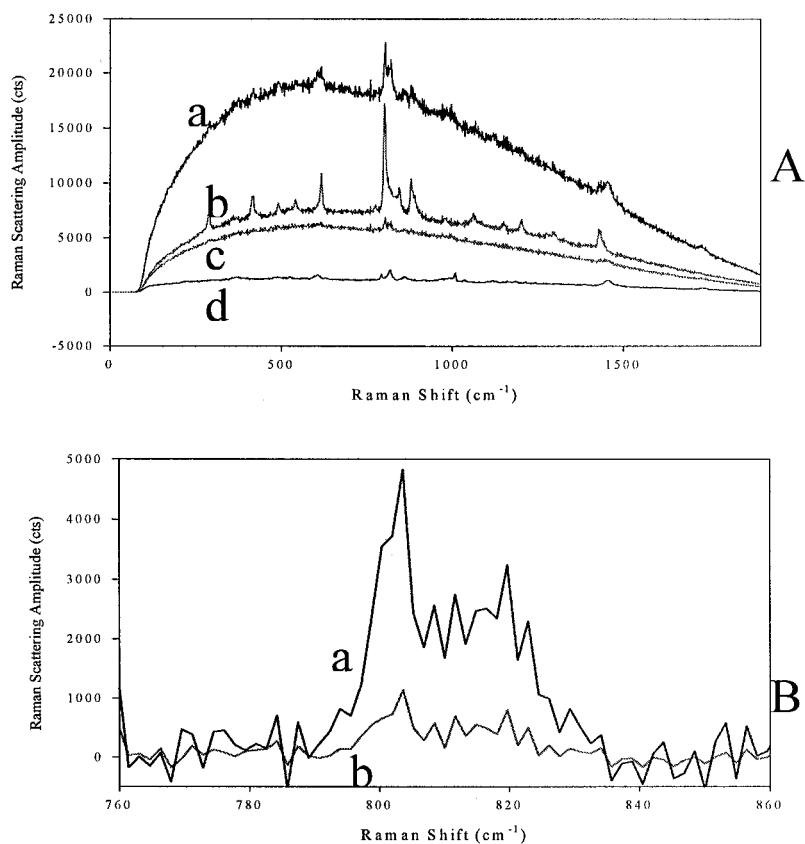


Figure 6. (A) Raman spectra for four samples: (a) surface side of the 50/50 blend film, (b) a pure film of PVDF, (c) interface side of the 50/50 blend film, and (d) a pure film of PMMA-co-PEA. (B) Comparison of the Raman spectra of the two sides of the 50/50 blend film over the range 760 – 860  $\text{cm}^{-1}$ : (a) surface side, (b) interface side.

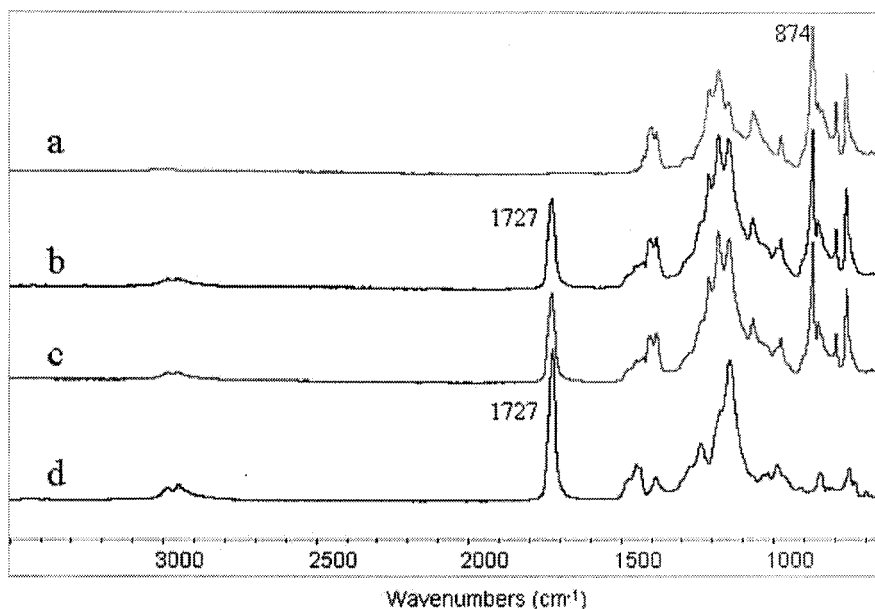


Figure 7. ATR-FTIR spectra for (a) a pure film of PVDF, (b) surface side of the 50/50 blend film, (c) interface side of the 50/50 blend film, and (d) a pure film of PMMA-co-PEA.

Fig. 7 shows ATR-FTIR spectra for the pure PVDF film (a), the pure PMMA-co-PEA film (d), the surface of the 50/50 blend film (b), and the interface of the 50/50 blend film (c). The band at  $1727\text{ cm}^{-1}$  is due to the stretching vibration of the C=O group in PMMA-co-PEA copolymer, while the intense absorption at  $874\text{ cm}^{-1}$  is a characteristic peak of PVDF that is assigned to  $\text{CH}_2$  rocking vibration of PVDF.<sup>20</sup> The intensity of the band at  $874\text{ cm}^{-1}$  is very weak in the pure PMMA-co-PEA, but it is enhanced dramatically in PVDF due to the existence of two fluorine atoms. The ratio between the intensity of the band at  $874\text{ cm}^{-1}$  ( $I_{874\text{ cm}^{-1}}$ ) and that at  $1727\text{ cm}^{-1}$  ( $I_{1732\text{ cm}^{-1}}$ ) is used to estimate the relative intensity of PVDF to PMMA-co-PEA for the two sides of different blends. The results are summarized in Table 1. The surfaces have higher  $I_{874\text{ cm}^{-1}}/I_{1732\text{ cm}^{-1}}$  values than the interfaces for all the three blends. Table 1 also displays the contact angle of  $\text{H}_2\text{O}$  and the surface polarity,  $X^p$ , which is the ratio between the polar force component and the total surface-free energy of the blend films. All the interface samples show a higher polarity than the corresponding surfaces. It should be mentioned that, contact angle is sensitive only to the first few angstroms of the surface layer and ATR-FTIR provides chemical information of a sample surface at a depth of approximately  $0.5\text{ }\mu\text{m}$  to  $2.0\text{ }\mu\text{m}$  by the diamond probe used in this study. Therefore, only chemical composition at or near the sample surface is presented in Table 1. The results of Table 1 clearly indicate that the surface samples contain higher PVDF material than the interface samples. The above difference in the chemical composition between the two sides of the blend films obtained by confocal Raman microscopy, ATR-FTIR and the contact angle measurement is consistent with their morphological difference obtained by AFM.

Table 1. Wettability and ATR-FTIR properties of the surface and the interface of different PMMA-co-PEA/PVDF blend films

PVDF / PMMA-co-PEA		$\theta_{\text{H}_2\text{O}}$ (°)	X <sup>P</sup>	I <sub>874 cm<sup>-1</sup></sub> / I <sub>1732 cm<sup>-1</sup></sub> (Before UV exposure)	I <sub>874 cm<sup>-1</sup></sub> / I <sub>1732 cm<sup>-1</sup></sub> (After UV exposure)
70/30	S	71.5 ± 0.9	0.21 ± 0.01	3.31	7.99
	I	58.3 ± 0.5	0.49 ± 0.02	3.08	8.11
50/50	S	72.5 ± 3.7	0.18 ± 0.05	1.91	3.32
	I	68.1 ± 4.7	0.38 ± 0.10	1.67	3.19
30/70	S	75.1 ± 1.4	0.16 ± 0.02	0.65	1.91
	I	63.5 ± 1.9	0.29 ± 0.03	0.53	1.23

### *After UV Exposure*

Table 1 also presents the ratios of I<sub>874 cm<sup>-1</sup></sub> to I<sub>1732 cm<sup>-1</sup></sub> for the samples after UV exposure for 7 months. Compared with the corresponding fresh samples, the intensity ratios of the exposed samples substantially increase, indicating a decrease of the acrylic copolymer on the sample surface after UV exposure. Chemical change due to UV exposure can be observed from the ATR-FTIR difference spectrum of 50/50 PVDF/PMMA-co-PEA surface sample (Fig. 8). Considering the possible variations in the contact area and, hence, the absorbance in the ATR-FTIR spectra, the band at 874 cm<sup>-1</sup> was used as an internal standard to obtain the difference spectrum. The peaks that decrease dramatically in the intensity in Fig. 8 are mostly associated with the PMMA-co-PEA copolymer, indicating that the acrylic copolymer has been degraded during the UV exposure. The chain scission with formation of low molecular mass gaseous products and limited monomer production would cause the mass losses of the acrylic copolymer in the sample.<sup>21,22</sup> The appearance of the peak around 1760 cm<sup>-1</sup> may be attributed to the anhydride or  $\gamma$ -lactone structures formed during the degradation of acrylic polymer.<sup>21</sup> Meanwhile, there is no obvious evidence to show a chemical change of PVDF after this period of UV exposure, because the characteristic bands that indicate chain crosslinking or chain scission of PVDF degradation (such as alkyne) are not visible in Fig. 8. From the above FTIR results, it is reasonable to suggest that chemical changes occurred on the sample surface is mainly by the degradation of the PMMA-co-PEA copolymer, with little chemical change in PVDF. However, additional research needs to be carried out to verify this conclusion.

UV degraded samples were also studied with AFM to determine the effect of UV exposure on the morphology and microstructure of the PVDF/PMMA-co-PEA blend films. For the surface of the 70/30 blend, there is no obvious change in the topography after UV exposure (Fig. 9). However, the phase images, especially the ones at a higher magnification (2  $\mu\text{m} \times 2 \mu\text{m}$ , Fig. 9b and Fig. 9d), have revealed that the microstructure of the spherulite has substantially changed after UV exposure for 7 months.

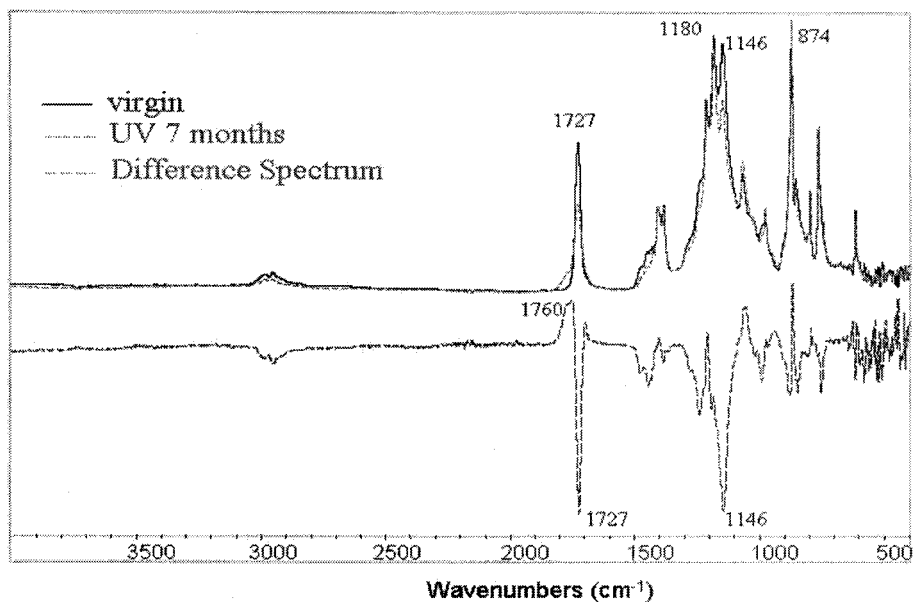


Figure 8. ATR-FTIR spectra of 50/50 PVDF/PMMA-co-PEA surface sample before and after UV exposure for 7 months. The difference spectrum is the subtraction of the spectrum of the virgin sample from the exposed one using  $874\text{ cm}^{-1}$  as an internal standard.

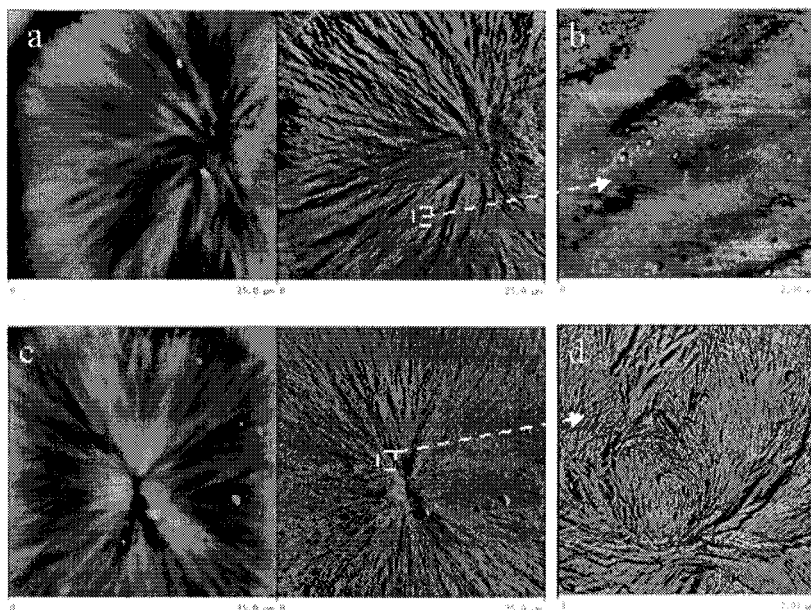


Figure 9. AFM images of the surface of the 70/30 PVDF/PMMA-co-PEA blend film: (a)  $25\text{ }\mu\text{m} \times 25\text{ }\mu\text{m}$  topographic (left) and phase (right) images, before UV exposure; (b) a higher magnification of the phase image of (a) in  $2\text{ }\mu\text{m} \times 2\text{ }\mu\text{m}$ ; (c)  $25\text{ }\mu\text{m} \times 25\text{ }\mu\text{m}$  topographic (left) and phase (right) images, after UV exposure; (d) a higher magnification of the phase image of (c) in  $2\text{ }\mu\text{m} \times 2\text{ }\mu\text{m}$ ; Contrast variation from black to white is  $400\text{ nm}$  for height image and  $90^\circ$  for phase image.

The distinct lamellae arrangements are clearly shown on the exposed sample, while blur branches with some amorphous particles are visible on the unexposed one. Similar morphological changes have been noticed on the surface of the 50/50 blend film as well (not shown). When the acrylic copolymer content increases to 70% in mass fraction, the height variation and surface roughness have substantially amplified after UV irradiation, with more apparent larger spherulite crystals observed in the AFM images (Fig. 10). This roughness change of the blend surface sample may relate to the gloss change reported previously for an acrylic-modified PVDF coating.<sup>23</sup> The change in the roughness is more pronounced for the interface samples than their corresponding surface samples after exposure at the same condition. As can be seen in the AFM images of the interface of the 70/30 PVDF/PMMA-co-PEA film (Fig. 11), the crystallites distinctly stick out on the sample surface, resulting in a much rougher surface than the unexposed one. Combining the ATR-FTIR and AFM results, it is reasonable to conclude that such morphological changes are due to a degradation of the acrylic copolymer on the surface and the interface of the blend films during UV exposure. The higher content of acrylic copolymer on the sample surface the more obvious changes were observed.

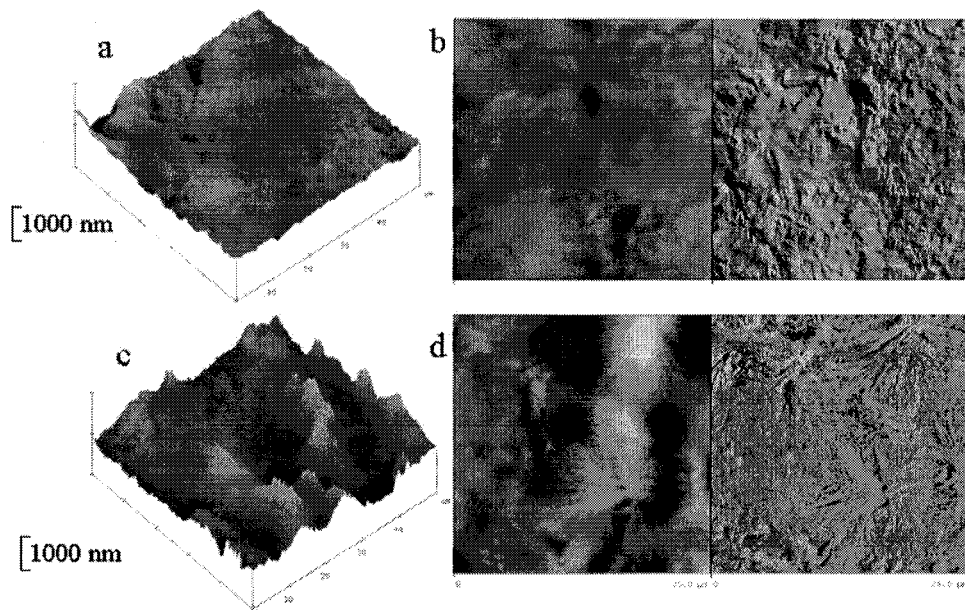


Figure 10. AFM images of the surface of the 30/70 PVDF/PMMA-co-PEA blend film: (a) 3-D topographic image, before UV exposure; (b) topographic (left) and phase (right) images, before UV exposure; (c) 3-D topographic image, after UV exposure; (b) topographic (left) and phase (right) images, after UV exposure. The scan size is 25  $\mu\text{m}$ . Contrast variation from black to white is 1000 nm for height image and 60  $^\circ$  for phase image.

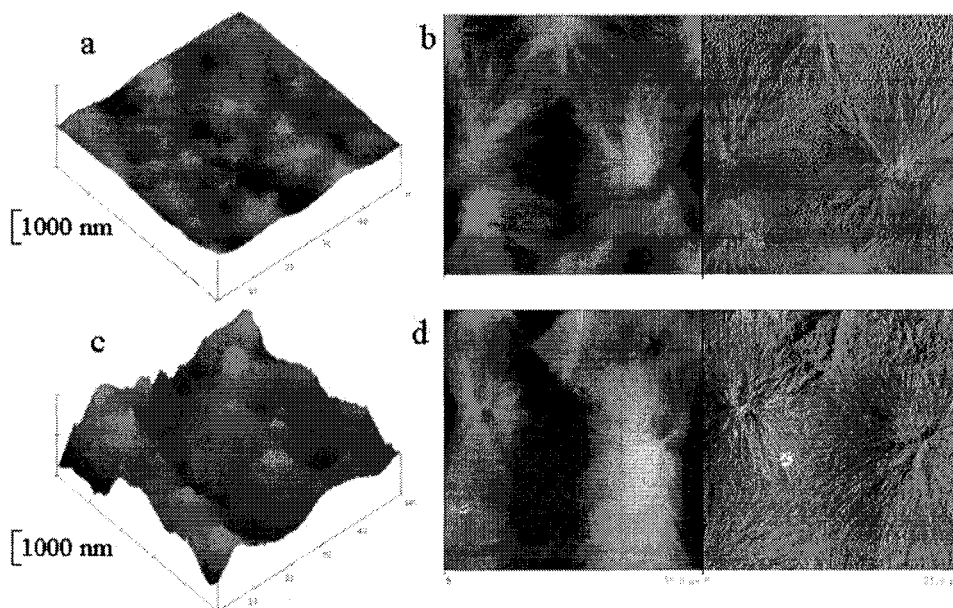


Figure 11. AFM images of the interface of the 70/30 PVDF/PMMA-co-PEA blend film: (a) 3-D topographic image, before UV exposure; (b) topographic (left) and phase (right) images, before UV exposure; (c) 3-D topographic image, after UV exposure; (d) topographic (left) and phase (right) images, after UV exposure. The scan size is 25  $\mu\text{m}$ . Contrast variation from black to white is 800 nm for height image and 60  $^\circ$  for phase image.

As seen in Fig. 9d, the fine lamellae organization in the spherulites is more clearly observed in the phase image of the exposed samples as compared to the unexposed ones. This structural change deserves some comments. The erosion of the acrylic copolymer during UV irradiation was probably mostly responsible for to the uncovering of the PVDF crystallites, revealing the detailed crystalline information without the interference of the acrylic material. However, it is also possible that the crystallite structure has been modified by the UV exposure. Previous studies have shown that PVDF can undergo recrystallization, increase its crystallinity or decrease the crystallinity by ionizing irradiation,  $\gamma$ -ray/UV exposure or thermal annealing.<sup>24-26</sup> The change depends on the parameters, such as radiation wavelength, the intensity and duration, temperature and environment. In this study, the UV exposure was performed at 50  $^\circ\text{C}$ , 9 % RH using UV source with the wavelength ranging from 275 nm to 800 nm. The exposure temperature was close to the glass temperature of the PVDF/PMMA-co-PEA blends (for example,  $T_g$  of 50/50 blend film is 53  $^\circ\text{C}$ ), and was much higher than  $T_g$  of PVDF (-70  $^\circ\text{C}$ ). The effect of the annealing and the UV irradiation may cause local movement, chain rearrangement, and even the recrystallization of PVDF in the blends. Therefore, the microstructural changes observed in the AFM images might not only be due to the degradation of acrylic copolymer in the blends but may also involve certain microstructural modifications in the PVDF crystalline. In order to elucidate those observations, further studies are being conducted with light scattering, neutron scattering, and X-ray scattering to examine if the crystal size and the crystallinity of the blends have been altered by the same exposure. The results will be presented in a future publication.

## Conclusions

Chemical and morphological properties of both the surface and the interface of PVDF/ PMMA-co-PEA blend films have been investigated by AFM, confocal Raman microscopy, ATR-FTIR and contact angle measurement before and after the samples were exposed to a xenon arch lamp at 50 °C and 9 % RH for 7 months. The results indicate that there are substantial differences between the surface and the interface of the blends. The air surfaces are enriched with PVDF, showing the spherulite crystallite structures. The interfaces are enriched with the acrylic copolymer. The amorphous materials dominate the morphology of the interface when the mass fraction of the acrylic polymer in the blend is approximately  $\geq 50\%$ . After UV exposure, significant degradation of PMMA-co-PEA copolymer has been observed on both the surface and the interface; however, little chemical change is noticed for the PVDF material. The surfaces of the blends having greater than 50 % mass fraction of PVDF show little change in the morphology after UV exposure. But for lower PVDF contents, a much rougher surface has been observed due to a larger amount of the erosion of the acrylic copolymer under the same exposure. Such roughness change should affect the gloss of coatings. Additionally, substantial change in the microstructure of the spherulites has been noticed after UV exposure. Well-organized lamellae structures are clearly observed in the phase image of the exposed samples as compared to the unexposed ones. The above change may be due to the erosion of PMMA-co-PEA copolymer on the sample surface and the microstructural modification of the crystallites in the PVDF spherulites. These results have great implications on the service life of PVDF-based coatings.

\*Certain commercial products or equipment are identified so as to specify adequately the experimental procedure. In no case does such identification imply recommendation or endorsement by NIST, nor does it imply that it is necessarily the best available for the purpose.

## References

1. Iezzi, R.A., Gaboury, S., and Wood, K. (2000), "Acrylic-fluoropolymer Mixtures and their Use in Coatings," *Prog. Org. Coat.*, 40, 55-60.
2. Iezzi, R.A. (1997), "Fluoropolymer Coatings For Architectural Application," *Modern Fluoropolymers*, John Wiley & Sons, 14, 271.
3. Anon. (1992), *Hylar 5000 technical brochure*, Ausimont USA Inc., PO Box 1838, Morristown, NJ 07962-1838, USA.
4. Scheirs, J., Burks, S., and Locaspi, A. (1995), "Development in Fluoropolymer Coatings," *Trends in Polymer Science*, 3, 74-82.
5. Bernstein, R.E., Crua, C.A., Paul, D.R., and Barlow, J.W. (1977), "LCST Behavior in Polymer Blends," *Macromolecules*, 10, 681-686.
6. Wang, T.T., and Nashi, T. (1977), "Spherulitic Crystallization In Compatible Blends of Poly(vinylidene fluoride) and Poly(methyl methacrylate)," *Macromolecules*, 10, 421-425.
7. Thomas, H.R., and Omalley, J.J. (1979), "Surface Studies On Multicomponent Polymer Systems By X-Ray Photoelectron-Spectroscopy- Polystyrene - Poly(ethylene oxide) Diblock Copolymers," *Macromolecules*, 12, 323-329.

8. Lee, W.K., Cho, W.J., Ha, C.S., Takahara, A., and Kajiyama, T. (1995), "Surface Enrichment of The Solution-Cast Poly(methyl methacrylate) Poly(vinyl acetate) Blends," *Polymer*, 36, 1229-1234.
9. Lee, W.K., and Ha, C.S. (1998), "Miscibility and Surface Crystal Morphology of Blends Containing Poly(vinylidene fluoride) by Atomic Force Microscopy," *Polymer*, 39, 7131-7134.
10. Ebbens, S.J., and Badyal, J.P.S. (2001), "Surface Enrichment of Fluorochemical-Doped Polypropylene Films," *Langmuir*, 17, 4050-4055.
11. Chen, X., McGurk, S.L., Davies, M.C., Roberts, C.J., Shakesheff, K.M., Tendler, S.J., and Williams, P.M. (1998), "Chemical and Morphological Analysis of Surface Enrichment in a Biodegradable Polymer Blend by Phase-Detection Imaging Atomic Force Microscopy," *Macromolecules*, 31, 2278-2283.
12. Wignall, G.D., and Wu, W.A. (1983), "SANS Investigation into the Role of Melting and Recrystallization During Solid-State Deformation of Polyethylene," *Polym. Commun.*, 24, 354-359.
13. Okabe, Y., Kyu, T., Saito, H., and Inoue, T. (1998), "Spiral Crystal Growth in Blends of Poly(vinylidene fluoride) and Poly(vinyl acetate)," *Macromolecules*, 31, 5823-5829.
14. Kalivianakis, P., and Jungnickel, B.J. (1998), "Crystallization-Induced Composition Inhomogeneities in PVDF/PMMA Blends," *J. Polym. Sci. Polym. Phys.*, 36, 2923-2930.
15. Brau, D., Jacobs, M., and Hellmann, G.P. (1994), "On the Morphology of Poly(vinylidene fluoride) crystals in blends," *Polymer*, 35, 706-17.
16. Briber, R.M., and Houry, F. (1987), "The Phase Diagram and Morphology of blends of Poly(vinylidene fluoride) and Poly(ethyl acrylate)," *Polymer*, 28, 38-42.
17. Magonov, S., and Godovsky, Y. (1999), "Atomic Force Microscopy, Part 8: Visualization of Granular Nanostructure in Crystalline Polymers," *American Laboratory*, 31(8), 52.
18. Sung, L., Gu, X., Landis, F.A., Ho, D.L., Nguyen, D., and Nguyen, T. "Effect of Processing Temperature on Microstructure and Physical property of PVDF-Acrylic blend films," *in preparation*.
19. Saito, H., Okada, T., Hamane, T., and Inoue, T. (1991), "Crystallization Kinetics in Mixtures of Poly(vinylidene fluoride) and Poly(methyl methacrylate): Two-Step Diffusion Mechanism," *Macromolecules*, 24, 4446-4449.
20. Boerio, F. J., and Koenig, J. L. (1969), *J. Polym. Sci. A-2*, 7, 1489.
21. Chiantore, O., Trossarelli, L., and Lazzari, M. (2000), "Photooxidation Degradation of acrylic and methacrylic Polymers," *Polymer*, 41, 1657-1668.
22. Torikai, A., Ohno, M., and Fueki, K. (1990), "Photodegradation of Poly(methyl methacrylate) By Monochromatic Light - Quantum Yield, Effect Of Wavelengths, and Light-Intensity," *J. Appl. Polym. Sci.*, 41, 1023-1032.
23. Wood, K.A., Headhli, L., and Willcox, P.J. (2002), "Patterns of Erosion from Acrylic and Fluoropolymer Coatings in Accelerated and Natural Weathering Tests," *J. Coating. Technol.*, 74 (924), 63-68.
24. Biswas, A., Gupta, R., Kumar, N., Avasthi, D.K., Singh, J.P., Lotha, S., Fink, D., Paul, S.N., and Bose, S.K. (2001), "Recrystallization in Polyvinylidene fluoride upon low fluence swift heavy ion impact," *Appl. Phys. Lett.*, 78, 4136-4138.
25. Pae, K.D., Bhateja, S.K., and Gilbert, J.R. (1987), "Increase in Crystallinity in Poly(vinylidene fluoride) by Electron Beam Radiation," *J. Polym. Sci., Polym. Phys.*, 25, 717-722.
26. Katan, E., Narkis, M., Siegmann, A. (1998), "The Effect of Some Fluoropolymers' Surfaces on Their Response to UV Irradiation," *J. Appl. Polym. Sci.*, 70, 1471-1481.